

# Numerical Evidence that the Singularity in Polarized $U(1)$ Symmetric Cosmologies on $T^3 \times R$ is Velocity Dominated \*

Beverly K. Berger

*Department of Physics, Oakland University, Rochester, MI 48309 USA*

Vincent Moncrief

*Departments of Physics and Mathematics, Yale University, New Haven, CT 06520 USA*

Numerical evidence supports the conjecture that polarized  $U(1)$  symmetric cosmologies have asymptotically velocity term dominated singularities.

98.80.Dr, 04.20.J

## I. INTRODUCTION

The cosmological singularity in spatially homogeneous models is known to be either asymptotically velocity term dominated (AVTD) (Kasner-like) [1,2] or Mixmaster-like [3,4]. Analytic [2,5] and numerical studies [6,7] have shown that the singularity in the spatially inhomogeneous Gowdy models [8] is AVTD everywhere in polarized models and everywhere except, perhaps, at a set of measure zero in the generic, unpolarized case. Long ago, Belinskii, Khalatnikov, and Lifshitz (BKL) [3] argued that the generic singularity in Einstein's equations is locally of the Mixmaster type. This remains controversial [9] but serves as a conjecture which can be tested. The Gowdy models, though interesting in their own right, have two commuting Killing fields which precludes local Mixmaster behavior for  $T^3 \times R$  topology. (For generalized Gowdy models which appear to exhibit Mixmaster dynamics see [10].) However, the more general one Killing field  $U(1)$  symmetric cosmologies on  $T^3 \times R$  should generically have Mixmaster-like singularities if the BKL conjecture is correct.

An AVTD solution to Einstein's equations is obtained by neglecting all terms containing spatial derivatives. The parameters of the solution to the resultant ODE's are then assumed to depend on the spatial coordinates. An AVTD singularity is then one where the solution to the full Einstein equations comes arbitrarily close to an AVTD solution as the singularity is approached [2]. For the  $U(1)$  cosmologies, the AVTD equations may be solved exactly. However, one may worry about the coordinate and slicing dependence of the notions of space and time leading to such dependence in our definition of AVTD. We shall argue here that the AVTD behavior of the singularity is not strongly slicing dependent.

We have already shown [6] that numerical methods used in the Gowdy cosmologies can be easily generalized to the  $U(1)$  case. However, numerical difficulties associated with spatial differencing in two dimensions have prevented so far a complete understanding of generic  $U(1)$  models probably because Gowdy-like spiky features [7] cannot yet be modeled with sufficient accuracy. However, the subclass of polarized  $U(1)$  models does not appear to develop spiky features and thus can be treated well by our numerical methods. We consider vacuum  $U(1)$  symmetric cosmologies on  $T^3 \times R$ . These can be described by two variables  $\varphi$  and  $\omega$  analogous to the Gowdy wave amplitudes for the  $+$  and  $\times$  polarizations of gravitational waves and three variables  $\Lambda$ ,  $x$ , and  $z$  which contain nondynamical information. Polarized  $U(1)$  models have the degree of freedom associated with  $\omega$  set equal to zero. This condition is preserved for all time both by Einstein's equations and by the discrete form thereof used in our numerical simulations. While a general solution to the initial value problem is not known explicitly, we have found an algebraic solution to the constraints which contains three (four for generic  $U(1)$  models) arbitrary functions of the spatial variables and is sufficiently general to yield generic evolution toward the singularity within the polarized  $U(1)$  class of models. We find that the evolution toward the singularity is AVTD everywhere as had previously been conjectured [11]. This conclusion is based (a) on the exponential decay with time of all terms in the Hamiltonian containing spatial derivatives, (b) the exponential decay with time of the change in certain functions of the spatial coordinates which are constant in time in the AVTD regime, and (c) fits of the behavior of the variables at randomly selected spatial points to the expected linear or constant asymptotic time dependence.

---

\*e-mail: berger@oakland.edu, moncrief@hepvms.physics.yale.edu

## II. THE MODEL

The spacelike Killing vector  $\xi = \partial/\partial x^3$  of the  $U(1)$  symmetry allows a generic metric in this class to be described in terms of the coordinate  $x^3$  along  $\xi$  and coordinates  $u$  and  $v$  and  $\tau$  parametrizing the quotient  $2+1$  manifold [12]. Using notation from [6] and taking  $u \in [0, 2\pi]$  and  $v \in [0, 2\pi]$  the  $3+1$  metric is

$$ds^2 = e^{-2\varphi} \{ -N^2 e^{-4\tau} d\tau^2 + e^{-2\tau} e^\Lambda e_{ab} dx^a dx^b \} + e^{2\varphi} (dx^3 + \beta_a dx^a)^2 \quad (1)$$

where  $\{x^a\} = \{u, v\} = \{x^1, x^2\}$ , the lapse  $N = e^\Lambda$ , and  $g_{ab} = e^\Lambda e_{ab}$  where

$$e_{ab} = \frac{1}{2} \begin{bmatrix} e^{2z} + e^{-2z}(1+x)^2 & e^{2z} + e^{-2z}(x^2-1) \\ e^{2z} + e^{-2z}(x^2-1) & e^{2z} + e^{-2z}(1-x)^2 \end{bmatrix} \quad (2)$$

is the conformal metric of the  $u$ - $v$  plane.

In the polarized case,  $\beta_a = 0$  but for the general case we must construct  $\{\beta_a\} = \{\beta_1, \beta_2\}$  as follows: At an initial time,  $\tau = \tau_0$ , define

$$\begin{aligned} \beta_1^*(u, v) &= c_1 + \int_0^v dv' \left\{ r(u, v') - \frac{1}{2\pi} \int_0^{2\pi} dv'' [r(u, v'')] \right\}, \\ \beta_2^*(u, v) &= c_2 - \frac{1}{2\pi} \int_0^u du' \int_0^{2\pi} dv' r(u', v') \end{aligned} \quad (3)$$

where  $c_1$  and  $c_2$  are constants. These constants are like “twist” constants [12] and are arbitrary (but physically significant). These  $\beta^*$ ’s will be periodic on  $T^2$  provided

$$\int_0^{2\pi} du \int_0^{2\pi} dv r(u, v) = 0. \quad (4)$$

Now let  $\beta_1 = \beta_1^* + \partial\lambda/\partial u$  and  $\beta_2 = \beta_2^* + \partial\lambda/\partial v$  where  $\lambda$  is arbitrary and could be identically zero to give  $\{\beta_a\}$  at  $\tau_0$ . Finally, define  $\beta_a(u, v, \tau)$  by computing

$$\beta_a(u, v, \tau) = \beta_a(u, v, \tau_0) - \int_{\tau_0}^\tau d\tau' e^{-2\tau'} N e^{-4\varphi} e_{ab} \varepsilon^{bc} \omega_{,c} \quad (5)$$

where

$$\varepsilon^{bc} = \begin{pmatrix} 0 & 1 \\ -1 & 0 \end{pmatrix}. \quad (6)$$

As in [12], a canonical transformation replaces the terms in the Einstein-Hilbert action  $e^a \dot{\beta}_a + \beta_0 e^a_{,a}$  by  $r \dot{\omega}$  where the momentum  $e^a$  conjugate to  $\beta_a$  identically satisfies the constraint  $e^a_{,a} = 0$  if  $e^a = \varepsilon^{ab} \omega_{,b}$ . Einstein’s equations may be obtained by the variation of

$$\begin{aligned} H &= \int \int du dv \mathcal{H} \\ &= \int \int du dv \left( \frac{1}{8} p_z^2 + \frac{1}{2} e^{4z} p_x^2 + \frac{1}{8} p^2 + \frac{1}{2} e^{4\varphi} r^2 - \frac{1}{2} p_\Lambda^2 + 2p_\Lambda \right) \\ &\quad + e^{-2\tau} \int \int du dv \left\{ (e^\Lambda e^{ab})_{,ab} - (e^\Lambda e^{ab})_{,a} \Lambda_{,b} + e^\Lambda [(e^{-2z})_{,u} x_{,v} - (e^{-2z})_{,v} x_{,u}] \right. \\ &\quad \left. + 2e^\Lambda e^{ab} \varphi_{,a} \varphi_{,b} + \frac{1}{2} e^\Lambda e^{-4\varphi} e^{ab} \omega_{,a} \omega_{,b} \right\} \\ &= H_K + H_V = \int \int du dv \mathcal{H}_K + \int \int du dv V. \end{aligned} \quad (7)$$

The Hamiltonian and momentum constraints are respectively

$$\mathcal{H}^0 = \mathcal{H} - 2p_\Lambda = 0 \quad (8)$$

and

$$\begin{aligned}\mathcal{H}^u &= p_z z_{,u} + p_x x_{,u} + p_\Lambda \Lambda_{,u} - p_{\Lambda,u} + p\varphi_{,u} + r\omega_{,u} + \frac{1}{2} \{ [e^{4z} - (1+x)^2] p_x - (1+x)p_z \}_{,u} \\ &\quad - \frac{1}{2} \{ [e^{4z} + (1-x^2)] p_x - x p_z \}_{,u} = 0,\end{aligned}\tag{9}$$

$$\begin{aligned}\mathcal{H}^v &= p_z z_{,v} + p_x x_{,v} + p_\Lambda \Lambda_{,v} - p_{\Lambda,v} + p\varphi_{,v} + r\omega_{,v} - \frac{1}{2} \{ [e^{4z} - (1-x)^2] p_x + (1-x)p_z \}_{,v} \\ &\quad + \frac{1}{2} \{ [e^{4z} + (1-x^2)] p_x - x p_z \}_{,v} = 0.\end{aligned}\tag{10}$$

To evolve Einstein's equations numerically, we need to solve the initial value problem. While an explicit general solution is not available, a particular class of solutions may be obtained as follows: To solve the momentum constraints (9) and (10) set  $p_x = p_z = \varphi_{,a} = \omega_{,a} = 0$  to leave  $p_\Lambda \Lambda_{,a} - p_{\Lambda,a} = 0$  which may be satisfied by requiring  $p_\Lambda = ce^\Lambda$ . For sufficiently large  $c$ , the Hamiltonian constraint may be solved algebraically for either  $p$  or  $r$ . In general, this leaves as free data the four functions  $x$ ,  $z$ ,  $\Lambda$ , and either  $r$  or  $p$ . However, in the polarized case, we demand

$$\omega = r = 0\tag{11}$$

so that the Hamiltonian constraint must be solved for  $p$  with three arbitrary functions  $x$ ,  $z$ , and  $\Lambda$ . We note that while any  $c$  will solve the initial value problem, to approach the singularity we require  $c > 0$  in order to give  $p_\Lambda > 0$  so that  $\Lambda$  will decrease (become more negative) as  $\tau \rightarrow \infty$ . This is required because the determinant of the metric has a factor  $e^{2\Lambda}$  which measures the area in the  $u$ - $v$  plane.

The AVTD equations may be obtained by variation of  $H_K$  in (7) and have the exact solution (see [6,13])

$$\begin{aligned}z &= -v_z(\tau - \tau_{0z}) + \ln[|\mu_z| (1 + e^{-4v_z(\tau - \tau_{0z}}))] \rightarrow -v_z\tau \quad \text{as } \tau \rightarrow \infty, \\ x &= \xi_z - \left[ \mu_z (1 + e^{-4v_z(\tau - \tau_{0z}}) \right]^{-1} \rightarrow x_0 \quad \text{as } \tau \rightarrow \infty, \\ p_z &= -4v_z \frac{(1 - e^{-4v_z(\tau - \tau_{0z}})}{(1 + e^{-4v_z(\tau - \tau_{0z}})} \rightarrow -4v_z \quad \text{as } \tau \rightarrow \infty, \\ p_x &= -\mu_z v_z \equiv p_x^0, \\ \varphi &= -v_\varphi(\tau - \tau_{0\varphi}) + \ln[|\mu_\varphi| (1 + e^{-4v_\varphi(\tau - \tau_{0\varphi}}))] \rightarrow -v_\varphi\tau \quad \text{as } \tau \rightarrow \infty, \\ \omega &= \xi_\varphi - \left[ \mu_\varphi (1 + e^{-4v_\varphi(\tau - \tau_{0\varphi}}) \right]^{-1} \rightarrow \omega_0 \quad \text{as } \tau \rightarrow \infty, \\ p &= -4v_\varphi \frac{(1 - e^{-4v_\varphi(\tau - \tau_{0\varphi}})}{(1 + e^{-4v_\varphi(\tau - \tau_{0\varphi}})} \rightarrow -4v_\varphi \quad \text{as } \tau \rightarrow \infty, \\ r &= -\mu_\varphi v_\varphi \equiv r^0, \\ \Lambda &= \Lambda_0 + (2 - p_\Lambda^0)\tau, \\ p_\Lambda &= p_\Lambda^0\end{aligned}\tag{12}$$

subject to the AVTD limit of the Hamiltonian constraint (8)

$$p_\Lambda^2 = \frac{1}{4}p_z^2 + e^{4z}p_x^2 + \frac{1}{4}p^2 + e^{4\varphi}r^2.\tag{13}$$

The AVTD limit is expressed in terms of  $\mu_z$ ,  $v_z \geq 0$ ,  $\xi_z$ ,  $\tau_{0z}$ ,  $\mu_\varphi$ ,  $v_\varphi \geq 0$ ,  $\xi_\varphi$ , and  $\tau_{0\varphi}$  which are functions of  $u$  and  $v$ . The limits on  $v_z$  and  $v_\varphi$  arise in order for the limiting forms of (12) to cause the exponents in (7) to decay as  $\tau \rightarrow \infty$ . (See the discussion of similar terms in Gowdy models [5,7].) The AVTD solution (12) may be inverted to give these parameters in terms of the original variables. Useful examples are

$$v_z = \sqrt{\frac{1}{16}p_z^2 + \frac{1}{4}e^{4z}p_x^2} \quad , \quad v_\varphi = \sqrt{\frac{1}{16}p^2 + \frac{1}{4}e^{4\varphi}r^2} \quad .\tag{14}$$

We further note [5] that, in addition to  $v_z$ ,  $v_\varphi$ ,  $p_x$ ,  $r$ , and  $p_\Lambda$ ,

$$c_z = \frac{1}{2}p_z + p_x x \quad , \quad c_\varphi = \frac{1}{2}p + r\omega\tag{15}$$

are also constant in time in an AVTD regime.

The method of Grubišić and Moncrief (GM) [5] can be followed to determine if one expects the singularity to be AVTD in the polarized model. We require every term in  $V$  (from (7)) to decay exponentially as  $\tau \rightarrow \infty$  if we substitute the limiting AVTD solution, (12), for the  $U(1)$  variables. Clearly, the behavior will depend on the behavior of the exponentials. First, as in the Gowdy case [5,7], we expect the remaining nonlinear term in  $\mathcal{H}_K$ ,  $e^{4z}p_x^2/2$  to drive  $p_z$  to negative values yielding  $z$  eventually large and negative. In that case, terms in  $e^{ab}$  proportional to  $e^{-2z}$  will dominate. From (7), we must examine the factor  $e^{-2\tau+\Lambda-2z}$  which will decay as  $\tau \rightarrow \infty$  if  $p_\Lambda - 2v_z > 0$ . (Recall that  $v_z \geq 0$ .) But the AVTD limiting form of the Hamiltonian constraint requires

$$p_z^2 + p^2 - 4p_\Lambda^2 = 0 = 16v_z^2 + p^2 - 4p_\Lambda^2 \quad (16)$$

which, in turn, requires  $p_\Lambda \geq 2v_z$ . Thus,  $p_\Lambda > 0$  is expected if the singularity is AVTD and yields consistent behavior.

### III. NUMERICAL METHODS

To integrate Einstein's equations, the symplectic method described in detail in [6] is applied to  $U(1)$  symmetric cosmologies. For a system described by a Hamiltonian

$$H = H_1 + H_2, \quad (17)$$

the corresponding evolution operator  $U(\Delta\tau)$  which evolves data from  $\tau$  to  $\tau + \Delta\tau$  generated by  $H$  can be written as [14,15]

$$U(\Delta\tau) = U_1\left(\frac{\Delta\tau}{2}\right)U_2(\Delta\tau)U_1\left(\frac{\Delta\tau}{2}\right) + \mathcal{O}[(\Delta\tau)^3] \quad (18)$$

where  $U_{1,2}$  are the evolution operators generated by  $H_{1,2}$ . Suzuki [16,17] has shown how to generalize this algorithm to an arbitrary order in  $\Delta\tau$ . This method is useful if the sets of equations of motion obtained by the separate variations of  $H_1$  and  $H_2$  are exactly solvable.

We see [6] that (7) for the  $U(1)$  models has exactly solvable equations for  $H_K$  and  $H_V$ . We have already obtained the AVTD solution (12) from  $H_K$ 's equations of motion. Since  $H_V$  contains no momenta, the configuration variables  $x$ ,  $z$ ,  $\Lambda$ ,  $\varphi$ , and  $\omega$  are constants of the motion so the equations are trivially solved. Non-trivial, however, is the representation of the gradients of  $V$  which arise during the variation. Accurate representation of spatial derivatives in two spatial dimensions is more difficult than in one dimension since the function of interest is no longer guaranteed to vary along the differencing direction. These inaccuracies have been found to limit the duration of *generic*  $U(1)$  model simulations *but are not problematical for polarized models*. This is almost certainly due to the fact that Gowdy-like, steepening spiky features characterized by increasingly (with  $\tau$ ) large spatial gradients are absent in polarized  $U(1)$  models as they also are in polarized Gowdy models. We emphasize that the ‘‘averaging’’ mentioned in [13] as necessary to stabilize generic  $U(1)$  evolution is not required in the polarized case.

To illustrate the behavior of typical polarized  $U(1)$  symmetric models, we consider a particular choice of initial data with  $\Lambda = A \sin u \sin v$ ,  $x = z = \cos u \cos v$ , and  $p_\Lambda = ce^\Lambda$  with  $A = 1$ ,  $c = 14$ . Other choices of initial data yield qualitatively similar results.

The constraints are imposed initially and monitored thereafter. Fig. 1 shows the maximum value of the constraints on the spatial grid vs time and spatial resolution. Although it is not clear how small one should require the constraints to be, the demonstrated convergence allows one to argue that the small constraint violation can be neglected in our interpretation of the results. Choptuik has argued that constraint convergence is an indicator of convergence of the numerical solution to the true solution to Einstein's equations [18].

### IV. RESULTS

Fig. 2 displays the maximum value of  $\log_{10} V$  from (7) at two spatial points as a function of  $\tau$ . One expects this quantity to vanish as  $\tau \rightarrow \infty$  for an AVTD singularity. Here we demonstrate that it vanishes exponentially as one expects. We note that the exponential decay of  $V$  measures only consistency and does not prove AVTD behavior. The observed exponential decay is compared to the predicted  $e^{(-p_\Lambda+p_z/2)\tau}$  behavior. While only representative spatial points have been shown, exponential decay at the predicted rate is seen at all spatial points.

In Fig. 3, the maximum values over the spatial grid of the *change* with time in the AVTD functions that should be constant in time in the AVTD limit— $p_x$ ,  $v_z$ ,  $v_\varphi$ ,  $c_z$ ,  $c_\varphi$ ,  $p_\Lambda$ —are plotted vs  $\tau$ . Again, one sees exponential decay to

the level of machine noise. (This machine noise does not show up in  $\log_{10} V$  which is an evaluation but does appear when differences are computed.) These quantities are strictly constant in the AVTD limit. In order to compare the observed to predicted decay of these quantities, one needs to go beyond the AVTD solution. In the Gowdy case, this was done by GM [5].

Finally, in Fig. 4, the variables  $\Lambda$ ,  $z$ , and  $\phi$ , expected to be linear with  $\tau$  in the AVTD limit, and  $x$  expected to be constant in  $\tau$  are shown vs  $\tau$  at typical spatial points. For the first three, linear fits are shown. We see that  $x$  does not show the constant in  $\tau$  behavior one would expect as  $\tau \rightarrow \infty$ . However, we note from Fig. 4 that  $x \approx 0$ . This small constant value allows the exponentially decaying term in  $x$  to be measurable. The lines in Fig. 4(d) are fit by a constant plus an exponential decaying with the expected rate of  $4v_z$  from (12). Again, although only representative points are displayed, the same behavior is seen at all spatial points.

## V. DISCUSSION

Numerical studies of polarized  $U(1)$  models provide strong evidence in support of their conjectured AVTD singularity. For a representative choice of initial data, all relevant terms are examined for consistency with AVTD behavior. Terms predicted to decay exponentially in the AVTD limit as  $\tau \rightarrow \infty$  do so with the expected slope. The terms  $c_z$ ,  $c_\varphi$ ,  $v_z$ ,  $v_\varphi$ ,  $p_x$ , and  $p_\Lambda$  are strictly constant in  $\tau$  for all  $\tau$  in the AVTD solution. Decay to the observed constant values could be compared with the prediction from the next order in an asymptotic expansion where the AVTD limit is the zero order term [5]. This has not been done. However, this is not required to demonstrate that the singularity is AVTD.

Given the consistency of our numerical results with the AVTD limit, we argue that longer duration simulations and other initial data sets will reveal nothing new. This is because the method of GM suggests that exponential decay of all the terms in  $V$  is consistent with the AVTD limit as  $\tau \rightarrow \infty$ . As shown in the Gowdy case [5] and, of course, in Mixmaster itself [3], the exponential growth of such terms is required to change the qualitative behavior of the model at a given spatial point. In the absence of this growth, there is no mechanism within Einstein's equations that could destroy the AVTD behavior.

Finally, we consider the possible slicing dependence of the notion of AVTD. First, we note that the canonical transformation to  $r$  and  $\omega$  has interchanged generalized coordinate and conjugate momentum. Of course, this degree of freedom is absent in polarized  $U(1)$  models. However the algebraic coordinate conditions which we have imposed in fixing the metric form (1) (essentially zero shift and a “harmonic” time function when the choice  $N = e^\Lambda$  is enforced) are not completely rigid since they depend still upon the choice of an initial hypersurface. There are many other harmonic time functions (i.e., solutions of the wave equation having timelike gradient) which could have been used instead of any given one without disturbing the metric form but one can analyze these asymptotically using the formal expansion methods of GM. This (not yet rigorously justified) analysis determines the asymptotic behavior of any such time function relative to a given one (with respect to which AVTD behavior of the metric is assumed) and shows that asymptotic velocity term dominance would be preserved in any harmonic time, zero shift gauge provided it holds in the original one. Thus the occurrence of AVTD behavior does not seem to depend upon the choice of a preferred initial hypersurface, at least not within the class of gauges under study.

## ACKNOWLEDGEMENTS

We would like to thank the Albert Einstein Institute at Potsdam for hospitality. This work was supported in part by National Science Foundation Grants PHY9507313 and PHY9503133. Numerical simulations were performed at the National Center for Supercomputing Applications (University of Illinois).

## FIGURE CAPTIONS

Figure 1. Convergence of the constraints. The Hamiltonian (triangles),  $u$ -momentum (circles), and  $v$ -momentum constraints vs  $\tau$  for spatial resolutions of  $128 \times 128$  (broken line),  $248 \times 248$  (solid line), and  $512 \times 512$  (dashed line). (a) A second order (in time) accurate symplectic PDE solver yields a decrease in the magnitude of the constraints by a factor of 4 as the number of spatial grid points in each direction is doubled (second order convergence). (b) A fourth order (in time) accurate symplectic PDE solver [16,17] yields a factor of 16 decrease in the magnitude of the constraints (fourth order convergence). Only the early part of the evolution is shown. Note that in addition to improvement in convergence with increasing spatial resolution, one also finds convergence with increasing time order accuracy. In all cases, the spatial differencing scheme [19] is fourth order accurate and centered about the spatial grid point of interest [18].

Figure 2. Exponential decay of the spatial derivative terms in the Hamiltonian.  $\log_{10} |V|$  vs  $\tau$  is displayed for two spatial points (solid line). The straight line slope indicates exponential decay. In each case, the corresponding values of  $(-p_\Lambda + p_z/2)\tau / \ln 10$  are also displayed (dashed line). Figures 2–5 are obtained from a second order accurate PDE solver with  $512^2$  spatial grid points.

Figure 3. Decay of the deviations from constant in time behavior of quantities constant in the AVTD limit. The maximum value of the change with time over the spatial grid of the quantities  $p_x$ ,  $c_z$ ,  $v_z$ ,  $c_\varphi$ ,  $v_\varphi$ , and  $p_\Lambda$  are shown vs  $\tau$ . The non-vanishing values at late times are at the level of machine precision errors.

Figure 4. Comparison of predicted and measured values of the variables (a)  $\Lambda$ , (b)  $z$ , (c)  $\varphi$ , and (d)  $x$  vs  $\tau$  are shown for two representative spatial points. For (a), (b), and (c), the data is represented by circles or squares while the solid line is a linear fit to the data. For (d), the fit is to  $x = a + be^{-p_z\tau}$  as is consistent with (12).

- 
- [1] Eardley, D., Liang, E., and Sachs, R., J. Math. Phys. **13**, 99 (1972).
  - [2] Isenberg, J. A. and Moncrief, V., Ann. Phys. (N.Y.) **199**, 84 (1990).
  - [3] Belinskii, V. A., Lifshitz, E. M., and Khalatnikov, I. M., Sov. Phys. Usp. **13**, 745 (1971).
  - [4] C. W. Misner, Phys. Rev. Lett. **22**, 1071 (1969).
  - [5] Grubišić, B. and Moncrief, V., Phys. Rev. D **47**, 2371 (1993).
  - [6] Berger, B. K. and Moncrief, V., Phys. Rev. D **48**, 4676 (1993).
  - [7] Berger, B. K. and Garfinkle, D., submitted to *Phys. Rev. D*, gr-qc/9710102.
  - [8] R. H. Gowdy, Phys. Rev. Lett. **27**, 826 (1971).
  - [9] Barrow, J. D. and Tipler, F., Phys. Rep. **56**, 372 (1979).
  - [10] Weaver, M., Isenberg, J., and Berger, B. K., submitted to *Phys. Rev. Lett.*, gr-qc/9712055.
  - [11] Grubišić, B. and Moncrief, V., Phys. Rev. D **49**, 2792 (1994).
  - [12] V. Moncrief, Ann. Phys. (N.Y.) **167**, 118 (1986).
  - [13] B. K. Berger, in *General Relativity and Gravitation*, edited by Francaviglia, M., Longhi, G., Lusanna, L., and Sorace, E. (World Scientific, Singapore, 1997), pp. 57–78.
  - [14] Fleck, J. A., Morris, J. R., and Feit, M. D., Appl. Phys. **10**, 129 (1976).
  - [15] V. Moncrief, Phys. Rev. D **28**, 2485 (1983).
  - [16] M. Suzuki, Phys. Lett. A **146**, 319 (1990).
  - [17] M. Suzuki, J. Math. Phys. **32**, 400 (1991).
  - [18] M. W. Choptuik, Phys. Rev. D **44**, 3124 (1991).
  - [19] A. H. Norton, U. of New South Wales preprint, 1992 (unpublished).

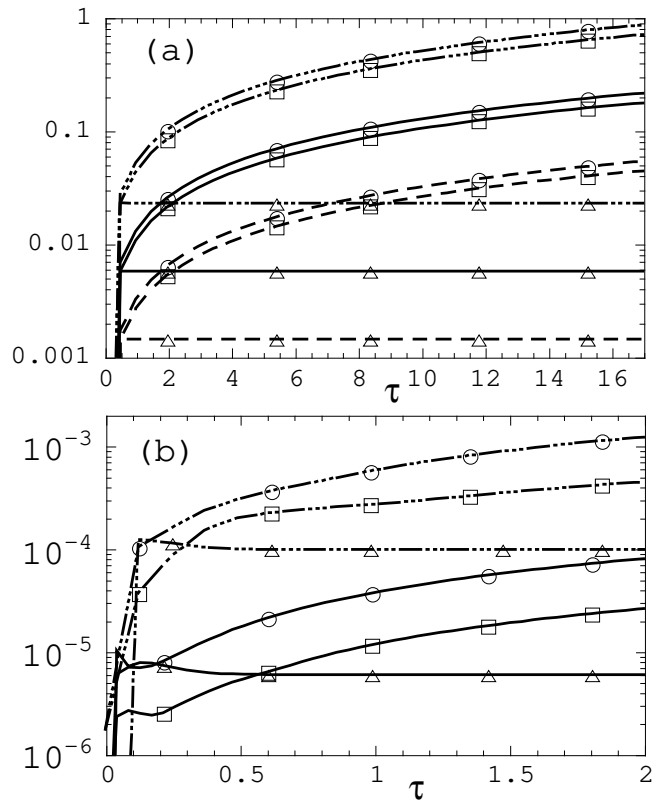


FIG. 1.

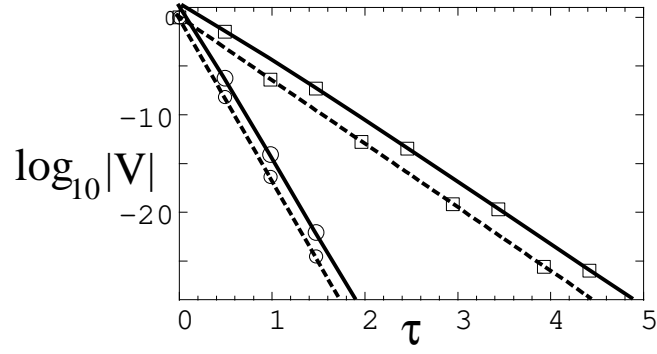


FIG. 2.

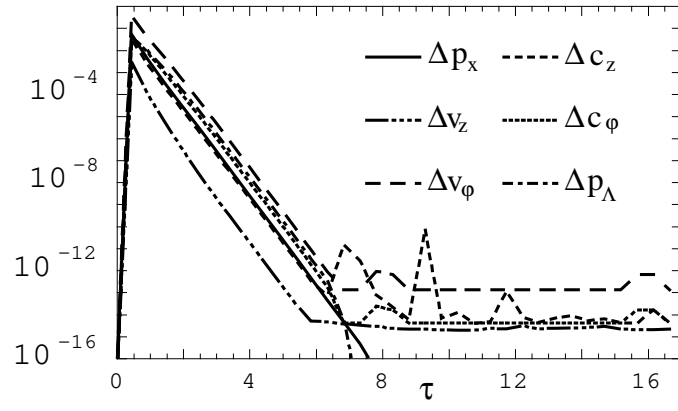


FIG. 3.

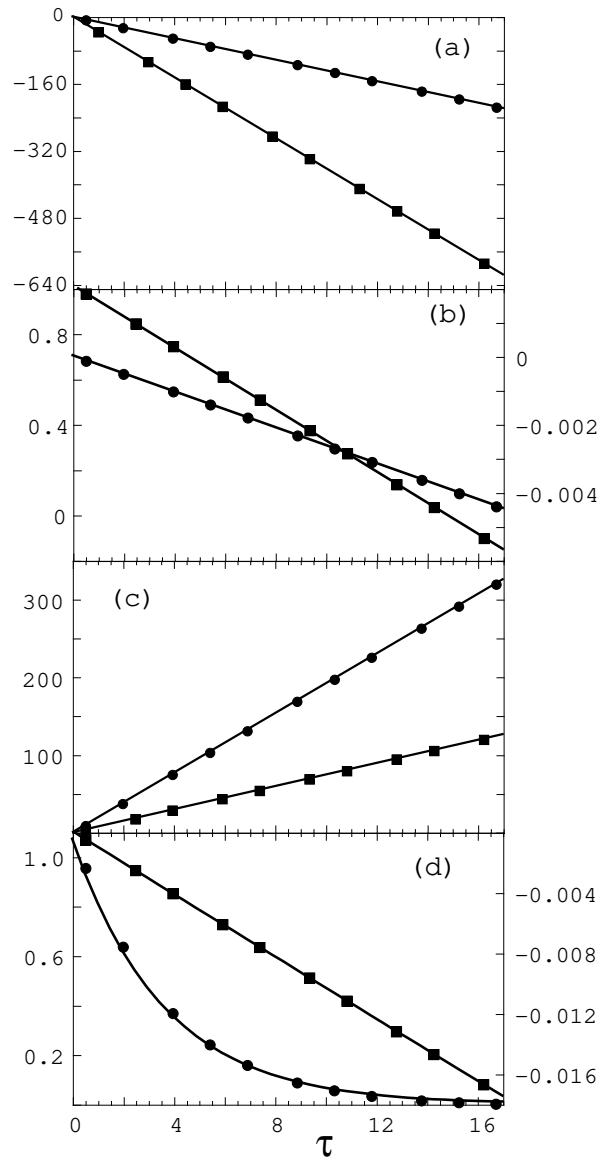


FIG. 4.